



## Adsorption in simple batch experiments of Coomassie blue G-250 by apricot stone activated carbon—Kinetics and isotherms modelling

Moussa Abbas<sup>a,\*</sup>, Abdelhamid Cherfi<sup>b</sup>, Samia Kaddour<sup>c</sup>, Tounsia Aksil<sup>b</sup>

<sup>a</sup>Laboratory of Soft Technologies and Biodiversity (LTDVPMBB), Faculty of Sciences, M'hamed Bougara University, 35000 Boumerdes, Algeria, Tel./Fax: +213 24911116; email: [moussaiap@gmail.com](mailto:moussaiap@gmail.com)

<sup>b</sup>Faculty of Sciences, Chemistry Department, M'hamed Bougara University, 35000 Boumerdes, Algeria, emails: [hcherfi@hotmail.com](mailto:hcherfi@hotmail.com) (A. Cherfi), [tounsiaiap@gmail.com](mailto:tounsiaiap@gmail.com) (T. Aksil)

<sup>c</sup>Laboratory of Macromolecular, Synthesis and Macromolecular Thio-Organic, Faculty of Chemistry, USTHB, BP 32-16111 El-Alia, Bab Ezzouar, Algeria, email: [mimakaddours@yahoo.fr](mailto:mimakaddours@yahoo.fr)

Received 18 November 2014; Accepted 23 June 2015

### ABSTRACT

The preparation of an activated carbon from apricot stones (ASAC) with H<sub>3</sub>PO<sub>4</sub> activation and its ability to remove the Coomassie blue (CB) from aqueous solutions are reported in this study. The spectroscopy method is used to get information on interactions between the functional groups of the adsorbent and the CB. Batch adsorption experiments were first undertaken to assess the effect of various parameters on the removal efficiency of CB. It was observed that under optimized conditions up to 98.022 mg/g could be removed from solution at 50°C. The equilibrium experimental data were analysed using Langmuir and Freundlich isotherm equations. An error-based statistic study showed that the isotherm data are well described by the Freundlich model. The suitability of the kinetic models for the adsorption of CB onto ASAC was also investigated. It was found that the adsorption kinetics of the dye obeyed pseudo-second-order kinetic model. The evaluation of thermodynamics parameters such as activation energy of adsorption ( $E_a$ : 66.161 kJ/mol) predicted the chemisorption nature of the sorption process. The negative Gibbs free energy ( $-\Delta G^\circ = 15.21$ – $19.27$  kJ/mol) and negative enthalpy change ( $\Delta H^\circ = -55.088$  kJ/mol) indicated, respectively, the spontaneous and exothermic nature of the reaction.

*Keywords:* Apricot stone; Coomassie blue G-250; Isotherm; Kinetics; Thermodynamics

### 1. Introduction

Dye production industries and many other industries which utilize dyes are increasing globally by the day with advancement in technology [1–3]. Textile, leather, paper, plastic, food, cosmetics, etc. are some of these industries. Presently, it was estimated that about 100,000 of different commercial dyes and pigments

exist and over 7.10<sup>5</sup> tonnes are produced annually worldwide [4,5]. As a result, water pollution by dyes has become one of the major pollution sources of the environment with approximately over 40,000 tonnes of dyes released every year into the environment [5,6]. Furthermore, most dyes are resistant to heat and light and are not biodegradable [5]. Their presence in wastewater causes the water pollution by lowering light penetration and photosynthesis [3]. Hence, the

\*Corresponding author.

removal of dyes from waste effluents has become environmentally important. Various processes have been investigated and shown to be effective in reducing dye concentrations in wastewater: chemical oxidation, biological treatment, coagulation–flocculation, membrane processes, adsorption, etc. [7,8]. Amongst these methods, the adsorption onto activated carbon has been found to be superior: inexpensive and effective to treat the wide range of dyes in wastewaters [5,7,8]. The high adsorption capacity of activated carbon is a result of its high surface area, extensive porosity in the interior of the particles, and presence of many different types of surface functional groups [5]. However, the available activated carbons in commerce are relatively expensive; their production and regeneration cost may constitute their limiting factors [6]. Hence, most researchers worldwide have focused on the search of new low-cost precursors especially issued from agricultural wastes. Precursors from wastes and agricultural by-products such as dolomite [8], date stones [9], waste bamboo scaffolding [5], wheat bran [10], bagasse [7], pumice and walnut [11], oil palm [12], lingo-cellulosic materials [13], date palm [14] and flamboyant pods [15] have shown potential. The objective of the present study was to use apricot stones as a low-cost precursor since agriculture in Algeria generates more than 20,000 tonnes of apricot stones each year, which represents a significant amount of solid pollutant. The aim of the study was to assess the ability of an activated carbon prepared from apricot stones for the removal of Coomassie blue (G-250), an acid dye largely used in the textile industry and commonly used in biology and biochemistry for staining proteins [16]. The study was carried out with the aim to optimize conditions for maximum removal of this dye from aqueous solutions. Besides this, the equilibrium adsorption data were fitted to various equations to obtain constants related to the adsorption phenomena. Finally, thermodynamic and kinetic studies were performed in order to investigate the adsorption process and estimate the rate of adsorption in parallel with thermodynamic parameters such as activation energy and changes in free energy, enthalpy and entropy.

## 2. Experimental

### 2.1. Materials and methods

Analytical grade reagents are used in all experiments. Acid dye, Coomassie blue (CB) (99%) is purchased from Merck Company. Chemical and physical properties of CB are listed in Table 1.

Table 1  
Chemical properties of acid dye, Coomassie blue (G-250)

Name	Coomassie brilliant blue (G-250)
Brute formula	$C_{47}H_{49}N_3NaO_7S_2$
Molecular weight	$(855.028 \pm 0.054)$ g/mol
Density	0.96 g/mL
Wave number ( $\lambda_{max}$ )	595 nm
Refractive index	1.334

Apricot stones obtained from Boumerdes region in Algeria, are air dried, crushed and screened to obtain two fractions with geometrical mean sizes ranging from 63  $\mu$ m to 2.5 mm. One hundred grams of the selected fraction are impregnated with concentrated  $H_3PO_4$  (85%) and subsequently subjected to carbonization and an activation process in a hot air oven at 250°C for 4 h. After, the produced activated carbon is cooled to room temperature, washed with distilled water to remove free acids until the pH reached 6.8 and then dried for 6 h at 105°C. Finally, the obtained biomass is grinded and sieved to get different particle sizes: <63, [63–80], [80–100], [100–200], [200–315], [315–800]  $\mu$ m and [0.8–1], [1–1.6], [1.6–2] mm.

### 2.2. Adsorption studies in batch mode

The effects of the experimental parameters such as, the initial CB concentration (10–100 mg/L), pH (2–10), adsorbent dosage (1–7 g/L) and temperature (295–329 K) on the adsorptive removal of CB ions were studied in a batch mode of operation for a specific period of contact time (0–60 min). ACB stock solution (1,000 mg/L) is prepared by dissolving the accurate amount of CB (99%) in distilled water. The CB solutions with required initial concentrations are prepared by diluting the stock solution and the pH is adjusted by adding solutions of HCl (0.1 M) or NaOH (0.1 M). For kinetic studies, desired quantity of ASAC is contacted with 10 mL of BC solutions in Erlenmeyer flasks. The flasks are then placed on a rotary shaker at 300 rpm and samples are taken at regular time intervals. Subsequently, the samples are centrifuged at 3,000 rpm for 10 min and the CB content in the supernatant is measured by a UV–vis spectrophotometer (Perkin Elmer model 550S) at its maximum wavelength of 595 nm.

The amount of CB ions adsorbed by activated carbon  $q_t$  (mg/g) is calculated using the following Eq. (1):

$$q_t = \frac{(C_0 - C_t) \cdot V}{m} \quad (1)$$

where  $C_0$  and  $C_t$  (mg/L) are the liquid-phase concentrations of CB at initial and a time  $t$ , respectively.  $V$  is the volume of the solution (L) and  $m$  is the mass of dry adsorbent used (g). Due to the inherent bias resulting from linearization of the adsorption isotherm models, a nonlinear regression by the root mean square error (RMSE) test was employed as criterion for the quality of fitting. The better accuracy of the theoretical models is obtained for the smallest values of RMSE [17]. The RMSE is evaluated by the following equation:

$$\text{RMSE} = \sqrt{\frac{1}{N-2} \cdot \sum_1^N (q_{e,\text{exp}} - q_{e,\text{cal}})^2} \quad (2)$$

where  $N$  is the number of experiments, while  $q_{e,\text{exp}}$  and  $q_{e,\text{cal}}$  are the experimental and calculated values of the CB uptake at equilibrium.

### 3. Results and discussion

#### 3.1. Structural characterization by infrared spectroscopy analysis

The Fourier transform infrared (FTIR) spectrum of ASAC, shown in Fig. 1, displays a number of absorption peaks, noticed around 3436, 2929, 1732, 1599 and 1508  $\text{cm}^{-1}$ , indicating that many functional groups of the adsorbent may be involved in the adsorption. The wide band between 3,122 and 3,680  $\text{cm}^{-1}$  is attributed to the hydroxyl ( $-\text{OH}$ ) groups (libber and intermolecular hydrogen band). The band at 2,929 and 1,508  $\text{cm}^{-1}$  suggest the presence of

( $-\text{CH}_2$ ) groups (symmetric and asymmetric), while the band at 1,599  $\text{cm}^{-1}$  indicates the presence of groups ( $\text{C}-\text{H}$ ,  $-\text{C}=\text{C}-$  and  $\text{C}=\text{C}$ ).

The peak at 1,732  $\text{cm}^{-1}$  is assigned to  $\text{C}=\text{O}$  in carboxylic groups. This clearly indicates that functional groups including carboxylic and hydroxyl groups contribute to CB adsorption on the binding sites.

#### 3.2. Effect of ASAC size

The effect of the ASAC particle sizes on the CB uptake efficiency was the first investigated amongst the series of batch experiments. As shown in Fig. 2, significant variations in uptake capacity were observed at different particles sizes; the best performance was obtained with particle sizes ranging in [315–800]  $\mu\text{m}$ . Indeed, generally the small particles provide a large surface area, which allows a high uptake capacity and removal efficiency. For the rest of the study, the [315–800]  $\mu\text{m}$  class was used in all adsorption experiments.

#### 3.3. Effect of pH

The pH of the CB solution plays an important role in the whole adsorption process and particularly on the adsorption capacity. As shown in Fig. 3(a), the uptake capacity of CB onto ASAC increases consistently with the decrease in pH. This effect of the pH may be explained on the basis of the pH of the point of zero charge ( $\text{pH}_{\text{pzc}}$ ) value at which the adsorbent is neutral. Under the  $\text{pH}_{\text{pzc}}$  value of the ASAC found to be 7.05 as shown in Fig. 3(b), the surface charge of the

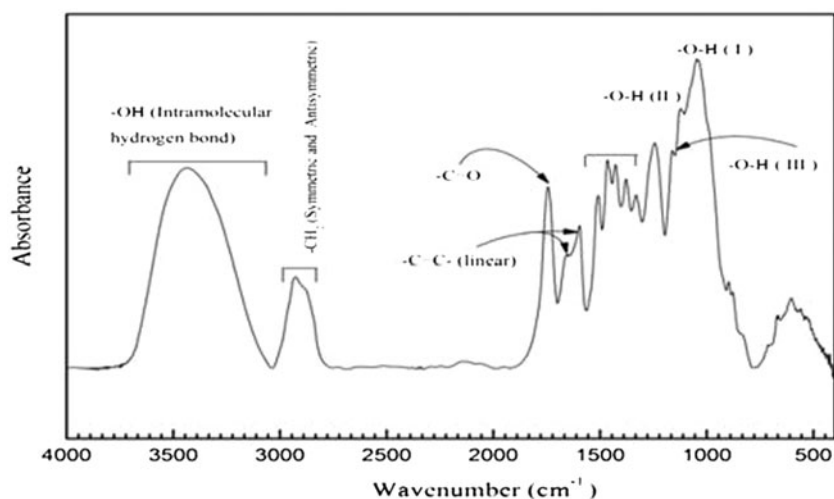


Fig. 1. Spectrum of FTIR analysis from ASAC.

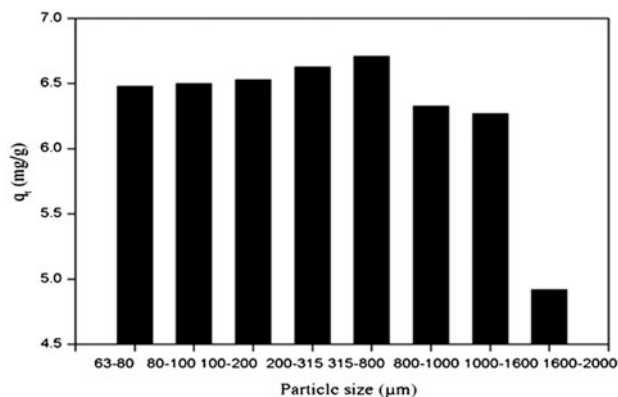


Fig. 2. Effect of particle size on the CB adsorption efficiency ( $T = 20^{\circ}\text{C}$ ,  $C_0 = 20 \text{ mg/L}$ , contact time = 45 min and stirring speed = 300 rpm).

adsorbent is positive [18] and consequently due to electrostatic attraction, the adsorption of CB anions is favoured. Indeed, the CB molecule presents differently charged states, corresponding to the amount of positive charges at the three nitrogen atoms present, while the two sulphonic acid groups are normally always negatively charged. Above pH 2, only one nitrogen atom carries a positive charge and the dye molecule is a blue anion with an overall charge of  $-1$ . Similar experimental details have been reported by Demirbas [19].

### 3.4. Effect of stirring speed

The effect of stirring speed on ASAC adsorption capacity is also investigated. Optimal value of adsorption capacity is obtained for a stirring speed of 300 rpm (Fig. 4). Such moderate speed gives a good homogeneity for the mixture suspension while high speeds, may lead to a swirling flow with surface vortex formation and poor solids distribution.

### 3.5. Effect of contact time and initial concentration

As shown in Fig. 5, for all studied concentrations, the adsorption capacity of CB increases with time and reaches a maximum value at 55 min indicating an equilibrium state, where no CB ions can be removed from the solution. It can also be concluded from Fig. 5 that when the initial concentration increases from 10 to 100 mg/L, the amount of CB adsorbed at equilibrium ( $q_e$ ) increases eightfold, from 8.09 to 66.17 mg/g indicating that the initial CB concentration plays an important role in the adsorption process. Indeed, the initial concentration provides the necessary driving force to overcome the resistances to the mass transfer of CB between the aqueous and solid phases.

### 3.6. Dosage effect of the adsorbent

The effect of the ASAC dosage on the removal of CB ions is shown in Fig. 6, where significant

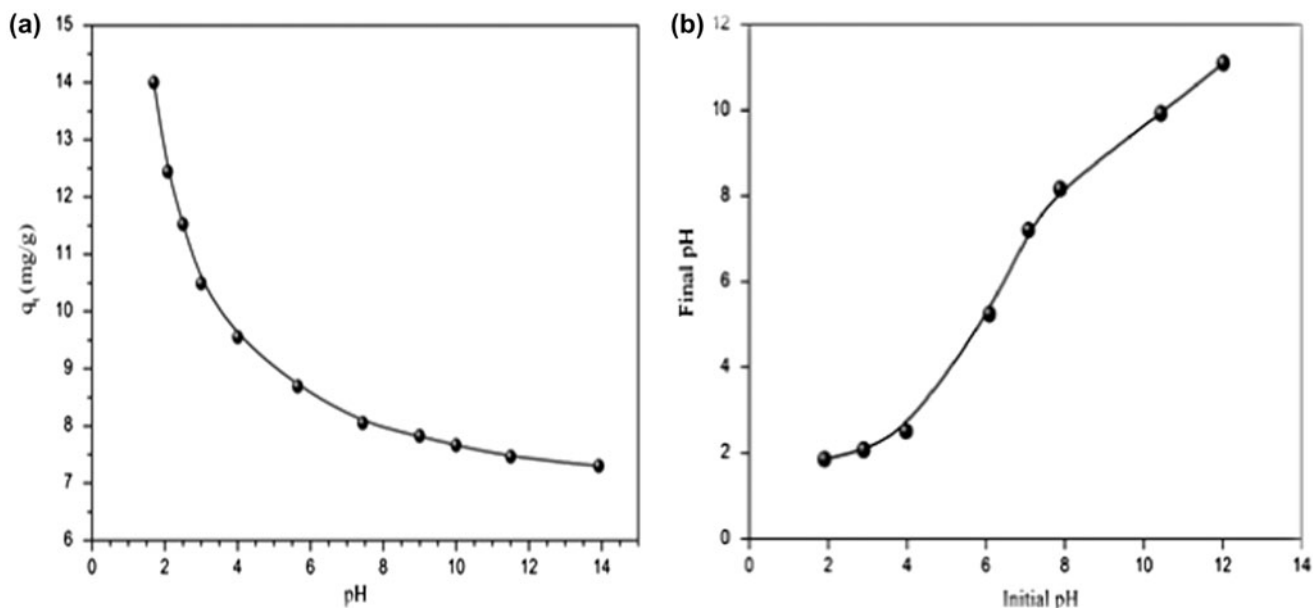


Fig. 3. (a) Effect of pH on the CB adsorption efficiency ( $T = 20^{\circ}\text{C}$ ,  $C_0 = 20 \text{ mg/L}$ , contact time = 45min, stirring speed = 300 rpm and particle size = [315–800 μm]) and (b) pH of the point of zero charge  $\text{pH}_{\text{pzc}}$  of the ASAC.

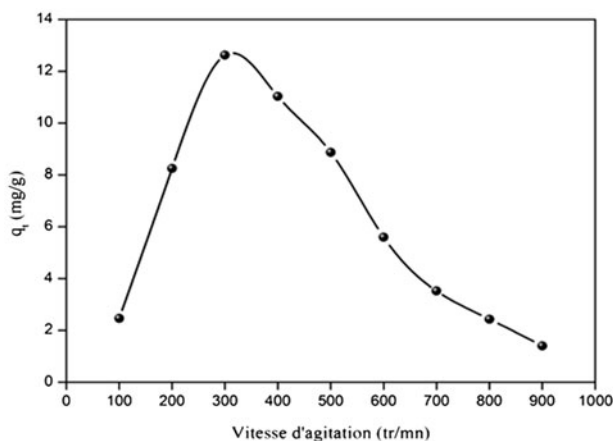


Fig. 4. Effect of stirring speed on the CB dye adsorption capacity ( $T = 20^\circ\text{C}$ ,  $C_0 = 20\text{ mg/L}$ , contact time: 45 min, pH 2 and particle size: [315–800  $\mu\text{m}$ ]).

variations in the uptake capacity can be observed at different adsorbent dosage (1–7 g/L). The best performance with a maximum removal of 39.55% is observed with a dosage of 7 g/L. This result was expected because by increasing the mass of the adsorbent, the contact surface and the active sites offered to the adsorbate increase, and therefore the removal efficiency increases too.

### 3.7. Adsorption isotherms

The shape of the isotherms is the first experimental tool to diagnose the nature of a specific adsorption phenomenon. The isotherms have been classified according to the classification of Giles et al. [20] in

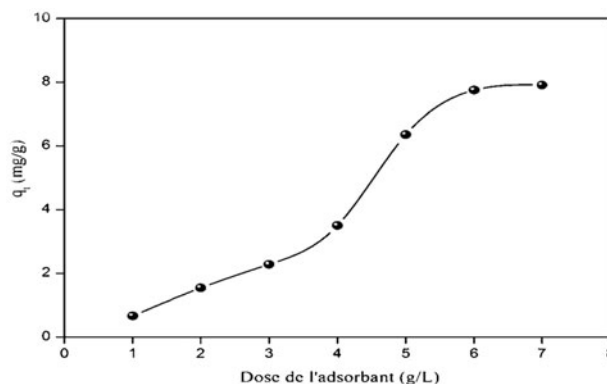


Fig. 6. Effect of adsorption dosage on the CB dye adsorption capacity ( $T = 20^\circ\text{C}$ ,  $C_0 = 20\text{ mg/L}$ , pH 2, particle size: [315–800  $\mu\text{m}$ ] and stirring speed = 300 rpm).

four main groups: L, S, H and C. According to the above classification, the isotherms of ASAC at different temperatures (22.5 and  $50^\circ\text{C}$ ) displayed an L curve pattern (Fig. 7). The initial part of the L curve indicates small interaction between acid dye and the carrier at low concentrations. However, as the concentration in the liquid phase increases, adsorption occurred more readily. This behaviour is due to a synergistic effect, with the adsorbed molecules facilitating the adsorption of additional molecules as a result of attractive adsorbate–adsorbate interactions.

Equilibrium relationships between adsorbent and adsorbate are described by adsorption isotherms.

Two adsorption isotherms are used in the present study namely, Langmuir [21] and Freundlich [22]. The applicability of the isotherm models to the adsorption study was compared by evaluating the statistic RMSE

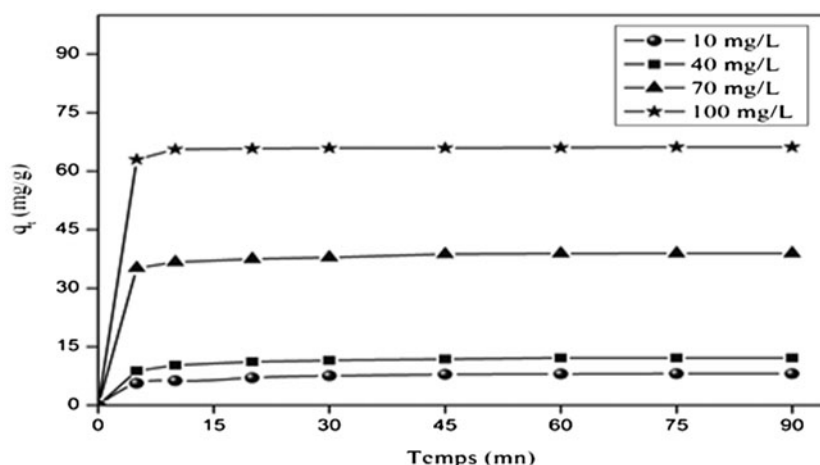


Fig. 5. Effect of the contact time on the adsorption of CB onto ASAC ( $T = 20^\circ\text{C}$ , pH 2, particle size = [315–800  $\mu\text{m}$ ]), stirring speed = 300 rpm and adsorbent dosage = 1.5 g/L).

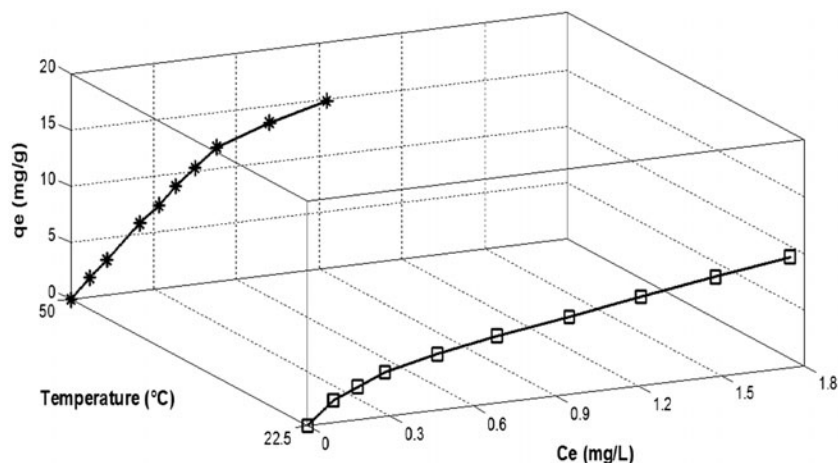


Fig. 7. Adsorption isotherms of CB by ASAC.

values. The linear forms of the Langmuir and Freundlich isotherms are represented by the following Eqs. (3) and (4) respectively:

$$\frac{1}{q_e} = \frac{1}{q_{max}} + \frac{1}{q_{max} \cdot K_L \cdot C_e} \tag{3}$$

where  $C_e$  is the equilibrium concentration (mg/L),  $q_e$  the amount of adsorbate adsorbed (mg/g),  $q_{max}$  the monolayer capacity (mg/g) and  $K_L$  is the Langmuir adsorption equilibrium constant (L/mg).

$$\ln q_e = \ln K_F + \frac{1}{n} \cdot \ln C_e \tag{4}$$

where  $K_F$  is a constant indicative of the adsorption capacity of the adsorbent (L/g) and  $n$  is an empirical constant related to the magnitude of the adsorption driving force.

The linearized Freundlich and Langmuir isotherms of CB at different temperatures (22.5 and 50 °C) are shown in Figs. 8 and 9 respectively.

The theoretical parameters of adsorption isotherms along with the regression coefficients are listed in Table 2. The smaller RMSE values obtained in Freundlich isotherms models indicate the better curve fitting.

The favourable nature of adsorption can be expressed in terms of dimensionless separation factor of equilibrium parameter, which is defined by Eq. (5) [23]:

$$R_L = \frac{1}{1 + K_L \cdot C_0} \tag{5}$$

where  $K_L$  is the Langmuir constant and  $C_0$  is the initial concentration of the adsorbate in solution. The values of  $R_L$  indicates the type of isotherm to be irreversible ( $R_L = 0$ ), favourable ( $0 < R_L < 1$ ), linear ( $R_L = 1$ ) or unfavourable ( $R_L > 1$ ). In this study, the  $R_L$  obtained values are less than 1, confirming that adsorption process is favoured in both the cases as well as applicability of Langmuir isotherm.

### 3.8. Adsorption kinetics

The kinetic study is important to an adsorption process because it describes the uptake rate of adsor-

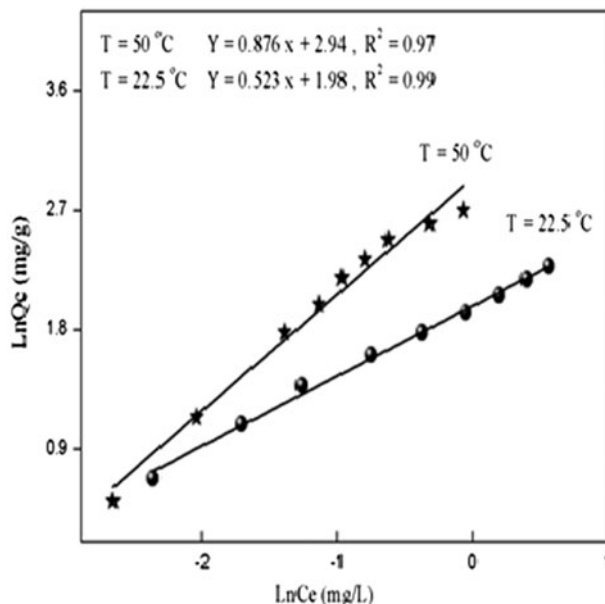


Fig. 8. Freundlich isotherms for the adsorption of CB ions onto ASAC.

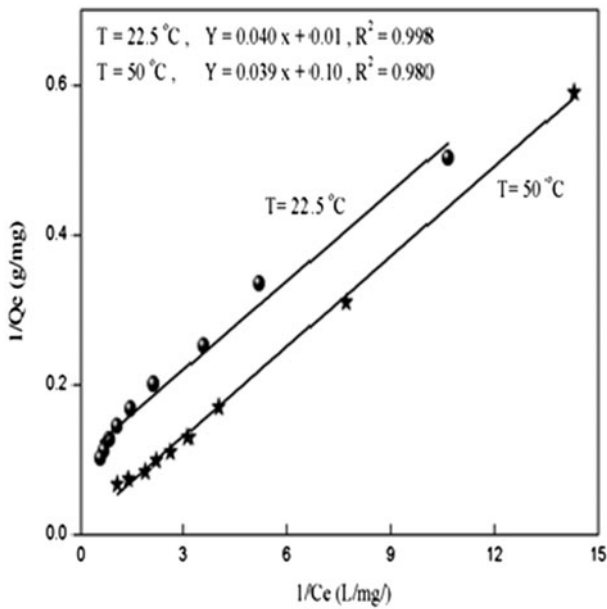


Fig. 9. Langmuir isotherms for the adsorption of CB ions onto ASAC.

bate, and controls the residual time of the whole adsorption process. Two kinetic models, pseudo-first-order and pseudo-second-order are selected in this study to describe the adsorption process. The pseudo-first-order equation is given below [24]:

$$\log(q_e - q_t) = \log q_e - \frac{k_1}{2.303} \cdot t \tag{6}$$

The pseudo-second-order model is given by Eq. (7) below [25,26]:

$$\frac{t}{q_t} = \frac{1}{k_2 \cdot q_e^2} + \frac{1}{q_e} \cdot t \tag{7}$$

where  $q_t$  (mg/g) is the amount of metal adsorbed on the adsorbent at various times  $t$  (min),  $k_1$  is the rate constant of pseudo-first-order kinetics ( $\text{min}^{-1}$ ),  $k_2$  is

the rate constant of the pseudo-second-order kinetic ( $\text{g/mg min}$ ). The rate constants, predicted uptakes and the correlation coefficients for ASAC are summarized in Table 3. For the pseudo-first-order kinetic, the experimental data deviated greatly from linearity (Fig. 10). This was evidenced by low  $q_e$  and low correlation value. Therefore, the pseudo-first-order model was inapplicable to this system. The correlation coefficient and the  $q_{e,cal}$  value from the pseudo-second-order kinetic model are seen to be in good agreement with the experimental results (Fig. 11).

The possibility of intraparticle diffusion during the transportation of adsorbate from solution phase to the surface of the adsorbent particles was also investigated using the intraparticle diffusion model given below by the formula (8) of Weber and Morris [27]:

$$q_t = K_{id} \cdot t^{1/2} + C \tag{8}$$

where  $K_{id}$  is the intraparticle diffusion rate constant ( $\text{mg/g min}^{1/2}$ ),  $q_t$  the amount of CB adsorbed at time  $t$  and  $C$  (mg/g) is the intercept. If intraparticle diffusion is rate limited then the plot of adsorbate uptake  $q_t$  vs. the square root of time ( $t^{1/2}$ ) would result in a linear relationship and  $K_{id}$  and  $C$  values can be obtained from these plot. The data collected at 22.5°C for an initial concentration of CB of 10 mg/L exhibit multilinear plots (two separate regions) (Fig. 12). This indicates that two steps occur during the adsorption process. The first step in diffusion model is the mass transfer of adsorbate molecules from the bulk solution to the adsorbent surface or instantaneous stage and second stage is the intraparticle diffusion on activated apricot stones. Moreover, the particle diffusion would be the rate-controlling step if the lines pass through the origin.

### 3.9. Effect of temperature

The activation energy  $E_a$  of the acid dye sorption was calculated using the Arrhenius equation (9) [28].

Table 2  
Sorption isotherm coefficients of Langmuir and Freundlich models

Langmuir $1/C_e = f(1/q_e)$	$T = 22.5^\circ\text{C}$		$T = 50^\circ\text{C}$		
	$T = 22.5^\circ\text{C}$	$T = 50^\circ\text{C}$	$T = 22.5^\circ\text{C}$	$T = 50^\circ\text{C}$	
$q_{max}$ (mg/g)	10.09	98.02	$1/n$	0.52	0.52
$K_L$ (L/mg)	2.46	0.25	$K_F$ (mg/g)	7.25	19.00
$R^2$	0.96	0.99	$R^2$	0.99	0.96
RMSE	0.45	1.93	RMSE	0.014	1.34

Table 3  
Kinetic parameters for adsorption of CB ions onto ASAC

$C_0$ (mg/L)	$q_{e,exp}$ (mg/g)	Pseudo-first-order kinetic			Pseudo-second-order kinetic		
		$k_1$ ( $\text{min}^{-1}$ )	$q_{e,cal}$ (mg/g)	$R^2$	$k_2$ (g/mg min)	$q_{e,cal}$ (mg/g)	$R^2$
10	8.09	0.0608	3.376	0.99	0.0389	8.389	0.99
40	12.14	0.0566	3.645	0.94	0.0318	12.583	0.99
70	38.72	0.0562	4.036	0.94	0.3644	39.200	0.99
100	66.18	0.0022	0.630	0.79	0.017	68.493	0.99

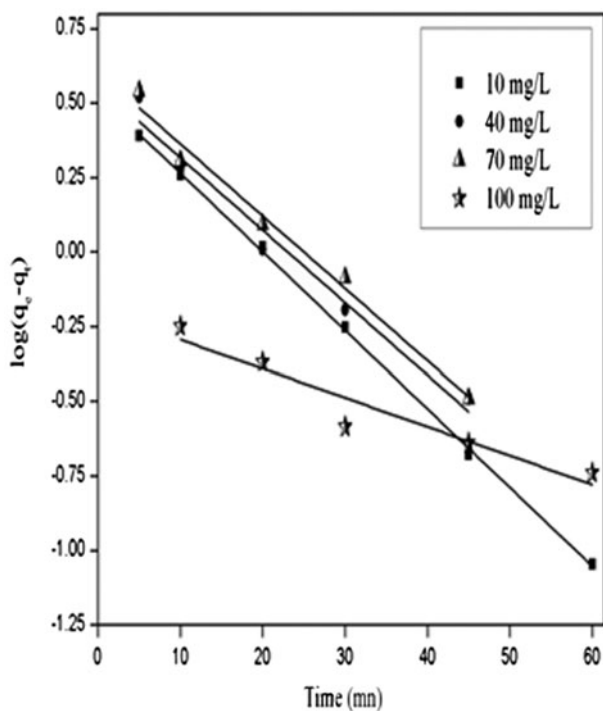


Fig. 10. First-order kinetic for the adsorption of CB onto ASAC.

$$\log k_2 = -\frac{E_a}{R \cdot T} + A \quad (9)$$

where  $A$  is the pre-exponential factor (g/mg min),  $R$  the universal gas constant (J/mol K),  $T$  the absolute temperature and  $k_2$  is the pseudo-second-order rate constant (g/mg min). The coefficient  $k_2$  has been determined at different temperatures using the pseudo-second-order kinetic model. The values obtained from the slopes of the plots  $t/q_t$  vs.  $t$  (Fig. 13) are consigned in Table 4. It is clear from the table that the value of  $k$  increases with the increase in temperature, indicating that sorption is favoured at high temperature.

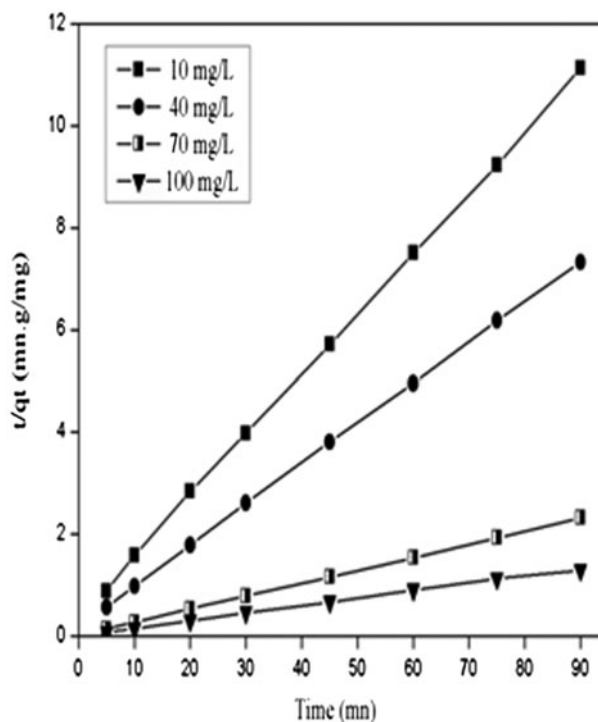


Fig. 11. Pseudo-second-order kinetic for the adsorption of CB onto ASAC.

The plot of  $\ln k_2$  vs.  $1/T$  gave a straight line as shown in Fig. 14, where the slope gives the activation energy  $E_a$  (66.161 kJ/mol), while the intercept indicates the pre-exponential factor  $A$  ( $\ln A = 20.187$  g/mg min). The magnitude of the activation energy gives an idea about the type of biosorption of CB onto ASAC. Indeed, the relatively high value found here belongs to the marge [60–800 kJ/mol] and consequently suggest that the phenomenon is mainly chemical.

Thermodynamic parameters, namely, free energy ( $\Delta G^\circ$ ), enthalpy ( $\Delta H^\circ$ ) and entropy ( $\Delta S^\circ$ ) changes were also calculated using Eqs. (10) and (11) and are given in Table 5.

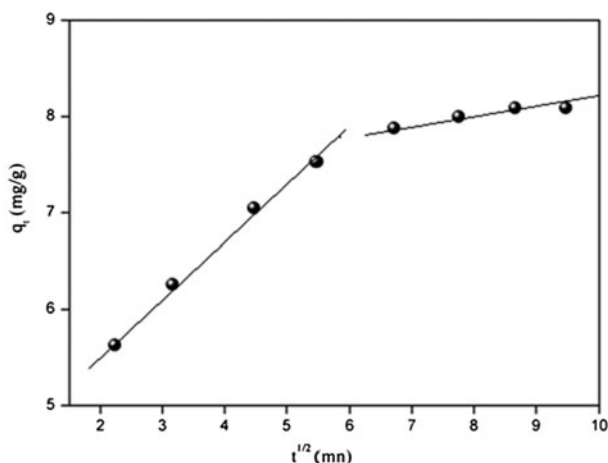


Fig. 12. Intraparticle diffusion plot for the adsorption of CB onto ASAC ( $T = 22.5^\circ\text{C}$ ,  $C_0 = 10\text{ mg/L}$  and adsorbent dosage =  $1\text{ g/L}$ ).

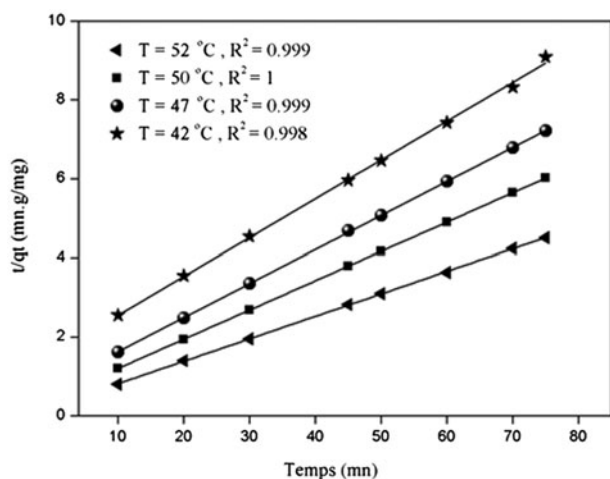


Fig. 13. Pseudo-second-order rate constant estimation for the adsorption of CB onto ASAC at different temperatures.

$$\Delta G^\circ = -RT \cdot \ln K_L \tag{10}$$

$$\Delta G^\circ = \Delta H^\circ - T \cdot \Delta S^\circ \tag{11}$$

Table 5  
Thermodynamic parameters for the CB adsorption on ASAC

T (K)	$K_L$ (L/mg)	$\Delta G^\circ$ (kJ/mol)	$\Delta H^\circ$ (kJ/mol)	$\Delta S^\circ$ (J/mol K)
295.5	2.55	-19.27	-55.088	121.209
329	0.26	-15.21		

Table 4  
The rate constant  $k_2$  at different temperatures

T ( $^\circ\text{C}$ )	$q_e$ (mg/g)	$k_2$ (g/mg min)	$R^2$
42	10.18	$6.10 \times 10^{-3}$	0.998
47	11.63	$9.64 \times 10^{-3}$	0.999
50	13.49	$11.90 \times 10^{-3}$	0.999
52	17.58	$13.12 \times 10^{-3}$	0.999

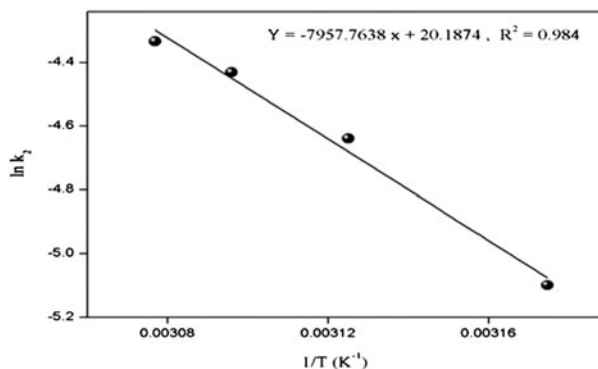


Fig. 14. A plot of  $\ln k_2$  against  $1/T$  for the adsorption of CB onto ASAC.

where  $K_L$  (L/mg) is the Langmuir constant,  $T$  the absolute temperature and  $R$  is the universal gas constant ( $8.134\text{ J/K mol}$ ).

The negative values of  $\Delta G^\circ$  and  $\Delta H^\circ$  indicate that the adsorption of CB onto ASAC is spontaneous and exothermic in the studied range of temperatures. The positive value of  $\Delta S^\circ$  states clearly that the randomness increased at the solid–solution interface during the CB adsorption onto the ASAC, indicating that some structural exchange may occur amongst the active sites of the sorbent and the ions.

### 3.10. Performance of the prepared ASAC

In order to have an idea about the efficiency of the prepared ASAC, a comparison of acid dye adsorption of this work and other relevant studies has been done as shown in Table 6. The adsorption capacity of the adsorbent  $q_{\max}$  was the parameter used for comparison. One can conclude that the value of  $q_{\max}$  in this

Table 6  
Comparison of ASAC performances with precursors from previous studies

Days	Adsorbents	$q_{\max}$ (mg/g)	Refs.
CBB	Apricot stones	98.021	This study
CBB	Coir pith	31.847	[29]
CBB	Wheat bran	6.4100	[10]
Basic yellow	Coffee ground	10.000	[30]
Methylene blue	Bamboo dust	143.20	[31]
Acid fuchsin	Sodium montmorillonite	93.240	[32]
Acid blue 45	Activated carbon cloth	65.460	[33]
Methylene blue	Palm kernel coat	277.77	[34]
Benzanil yellow	Bentonite	40.50	[35]
Benzanil yellow	Kaolin	30.60	[35]
Methylene blue	Carbon nano tube		[36]
	$T = 290$ K	103.62	
	$T = 300$ K	109.31	[36]
	$T = 310$ K	119.70	[36]
Methyl green	Activated carbon	30.700	[37]
Astrazon yellow	Apricot stone	211.23	[38]
Methylene blue	Strychnopotatorium seed	100.00	[39]
Methylene blue	Coconut shell fibres	19.59	[40]
Methylene blue	Olive stones	303.0	[41]
Methylene blue	Cotton waste	240.0	[42]
Methylene blue	Datepits	80.30	[43]
Methylene blue	Zeolite	53.10	[44]
Methyl orange	Camel thorn plant	20.830	[45]
Congo red	Activated carbon	35.210	[46]
Methylene blue	Activated carbon	194.73	[46]
Congo red	Lignin-based activated carbons	812.50	[47]
Basic blue 3	Agricultural waste	227.27	[2]

study is in good agreement than those in most of previous works which suggests that CB could be easily adsorbed by ASAC used in this work. This indicates that the apricot stone, very abundant in Algeria, is a type of cheap and effective adsorbent for the CB.

#### 4. Conclusions

This study has shown that activated carbon prepared from apricot stones can be employed as an effective adsorbent for the removal of CB ions from aqueous solution. Under optimized conditions, the maximum adsorption capacity was 10.04 mg/g at 22.5°C and 98.04 mg/g at 50°C. The Freundlich isotherm model provided a better fit of the equilibrium adsorption data than the Langmuir model, while the pseudo-second-order kinetic equation gave the best description of the kinetic data. The negative values of  $\Delta G^\circ$  and  $\Delta H^\circ$  indicated that the adsorption of CB onto ASAC is spontaneous and exothermic in the studied range of temperatures. The evaluation of the activation energy of adsorption ( $E_a = 66.161$  kJ/mol) predicted that the fixation of the dye on the adsorbent surface is

controlled by chemisorption, meaning that the CB ions form chemicals bonds with functional groups of the adsorbent.

#### References

- [1] B.H. Hameed, A.L. Ahmad, K.N.A. Latiff, Adsorption of basic dye (methylene blue) onto activated carbon-prepared from rattan sawdust, *Dyes Pigm.* 75 (2007) 143–149.
- [2] B.H. Hameed, F.B.M. Daud, Adsorption studies of basic dye on activated carbon derived from agricultural waste: Heveabrsiliensis seed coat, *Chem. Eng. J.* 139 (2008) 48–55.
- [3] P. Waranusantigul, P. Pokethitiyook, M. Kruatrachue, E.S. Upatham, Kinetics of basic dye (methylene blue) biosorption by giant duckweed (*Spirodela polyrrhiza*), *Environ. Pollut.* 125 (2003) 385–392.
- [4] T. Robinson, G. McMullan, R. Marchant, P. Nigam, Remediation of dyes in textile effluent: A critical review on current treatment technologies with a proposed alternative, *Bioresour. Technol.* 77 (2001) 247–255.
- [5] L.S. Chan, W.H. Cheung, S.J. Allen, G. McKay, Error analysis of adsorption isotherm models for acid dyes onto bamboo derived activated carbon, *Chin. J. Chem. Eng.* 20(3) (2012) 535–542.

- [6] M. Auta, B.H. Hameed, Preparation of waste tea activated carbon using potassium acetate as an activating agent for adsorption of acid Blue 25 dye, *Chem. Eng. J.* 171 (2011) 502–509.
- [7] M. Valix, W.H. Cheung, G. McKay, Preparation of activated carbon using low temperature carbonisation and physical activation of high ash raw bagasse for acid dye adsorption, *Chemosphere* 56 (2004) 493–501.
- [8] G.M. Walker, L. Hansen, J.A. Hanna, S.J. Allen, Kinetics of a reactive dye adsorption onto dolomitic orbents, *Water Res.* 37 (2003) 2081–2089.
- [9] S.K. They dan, M.J. Ahmed, Optimization of preparation conditions for activated carbons from date stones using response surface methodology, *Powder Technol.* 224 (2012) 101–108.
- [10] S. Ata, M.I. Din, A. Rasool, I. Qasim, I. Ul Mohsin, Equilibrium, thermodynamics, and kinetic sorption studies for the removal of Coomassie brilliant blue on wheat bran as a low-cost adsorbent, *J. Anal. Methods Chem.* 2012 (2012) 1–8.
- [11] B. Heibati, S. Rodriguez, A. Amrane, Uptake of Reactive Black 5 by pumice and walnut activated carbon: Chemistry and adsorption mechanisms, *J. Ind. Eng. Chem.* 20(5) (2014) 2939–2947.
- [12] M. Rafatullah, T. Ahmed, A. Ghazali, Oil palm biomass as a precursor of activated carbons: A review, *Crit. Rev. Env. Sci. Technol.* 43(11) (2013) 1117–1161.
- [13] L.W. Low, T.T. Teng, N. Morad, Adsorption studies of methylene blue and malachite green from aqueous solutions by pretreated lignocellulosic materials, *Sep. Sci. Technol.* 48(11) (2013) 1688–1698.
- [14] T. Ahmed, M. Danish, A. Ghazali, The use of date palm as a potential adsorbent for wastewater treatment: A review, *Environ. Sci. Pollut. Res.* 19(5) (2012) 1464–1484.
- [15] A.M.M. Vargas, A.L. Cazetta, A.C. Martins, J.C.G. Moraes, E.E. Garcia, G.F. Gauze, W.F. Costa, V.C. Almeida, Kinetic and equilibrium studies: Adsorption of food dyes acid Yellow 6, acid Yellow 23 and acid Red 18 on activated carbon from flamboyant pods, *Chem. Eng. J.* 181–182 (2012) 243–250.
- [16] N. Carlsson, C.C. Kitts, B. Akerman, Spectroscopic characterization of Coomassie blue and its binding to amyloid fibrils, *Anal. Biochem.* 420 (2012) 33–40.
- [17] M. Abbas, S. Kaddour, M. Trari, Kinetic and equilibrium studies of cobalt adsorption on apricot stone activated carbon, *J. Ind. Eng. Chem.* 20(3) (2014) 745–751.
- [18] Lj.S. Cerovic', S.K. Milonjic', M.B. Todorovic', M.I. Trtanj, Y.S. Pogozhev, Y. Blagoveschenskii, E.A. Levashov, Point of zero charge of different carbides, *Colloid Surf. A* 297 (2007) 1–6.
- [19] E. Demirbas, Adsorption of cobalt(II) ions from aqueous solution onto activated carbon prepared from hezelmüt shells, *Adsorpt. Sci. Technol.* 21(10) (2003) 951–963.
- [20] C.H. Giles, T.H. Ewan Mac, S.N. Nakhwa, D. Smith, Studies in adsorption. Part XI. A system of classification of solution adsorption isotherms, and its Use in diagnosis of adsorption mechanisms and in measurement of specific surface areas of solids, *J. Chem. Soc.* 10 (1960) 3973–3993.
- [21] I. Langmuir, The adsorption of gases on plane surfaces of glass, mica and platinum, *J. Am. Chem. Soc.* 40 (1918) 2221–2295.
- [22] H.M.F. Freundlich, Over the adsorption in solution, *J. Phys. Chem.* 57 (1906) 385–470.
- [23] K.R. Hall, L.C. Eagleton, A. Acrivos, T. Vermeulen, Pore- and solid-diffusion kinetics in fixed-bed adsorption under constant-pattern conditions, *Ind. Eng. Chem. Fundam.* 5 (1966) 212–223.
- [24] S. Lagergren, About the theory of so-called adsorption of soluble substances, *K. Sven. Ventenskapsakad. Handlingar* 24 (1998) 1–39.
- [25] Y.S. Ho, G. Mc Kay, The kinetics of sorption of divalent metal ions onto sphagnum moss peat, *Water Res.* 34(3) (2000) 735–742.
- [26] Y.S. Ho, G. Mc Kay, Pseudo-second order model for sorption processes, *Process Biochem.* 34(5) (1999) 4513–4513.
- [27] W.J. Weber, J.C. Morris, Kinetics of adsorption on carbon from solution, *J. Sanitary Eng. Div. Am. Soc. Chem. Eng.* 89 (1963) 31–59.
- [28] A. Tassist, H. Lounici, N. Abdi, N. Mameri, Equilibrium, kinetic and thermodynamic studies on aluminum biosorption by a mycelial biomass (*Streptomyces rimosus*), *J. Hazard. Mater.* 183(1–3) (2010) 35–43.
- [29] R. Naveen Prasad, S. Viswanathan, J. Renuka Devi, J. Rajkumar, N. Parthasarathy, Kinetics and equilibrium studies on biosorption of CBB by coir pith. *Am.-Eurasian J. Sci. Res.* 3(2) (2008) 123–127.
- [30] A. Namane, A. Mekarzia, K. Benrachedib, N. Belhaneche-Bensemra, A. Hellal, Determination of the adsorption capacity of activated carbon made from coffee grounds by chemical activation with  $ZnCl_2$  and  $H_3PO_4$ , *J. Hazard. Mater.* B119 (2005) 189–194.
- [31] N. Kannan, M.M. Sundaram, Kinetics and mechanism of removal of methylene blue by adsorption on various carbons—A comparative study, *Dyes Pigm.* 51 (2001) 25–40.
- [32] A.S. Elsherbiny, Adsorption kinetics and mechanism of acid dye onto montmorillonite from aqueous solutions: Stopped-flow measurements, *Appl. Clay Sci.* 83–84 (2013) 56–62.
- [33] N. Hoda, E. Bayram, E. Ayranci, Kinetic and equilibrium studies on the removal of acid dyes from aqueous solutions by adsorption onto activated carbon cloth, *J. Hazard. Mater.* B137 (2006) 344–351.
- [34] N.A. Oladoja, C.O. Aboluwoye, Y.B. Oladimeji, Kinetic and isotherm studies of MB adsorption onto ground palm kernel coat Turkish, *J. Eng. Env. Sci.* 32 (2008) 303–312.
- [35] B. Benguella, A. Yacouta-Nour, Elimination des colorants acides en solution aqueuse par la bentonite et le Kaolin (Removal of acid dyes from aqueous solutions using bentonite and kaolin), *C.R. Chim.* 12(6) (2009) 762–771.
- [36] Z. Hardryari, A.S. Goharrizi, M. Azadi, Experimental study of methylene blue adsorption from aqueous solutions onto carbon nano tubes, *Int. J. Water Res. Environ. Eng.* 2(2) (2010) 16–28.
- [37] O. Baghriche, K. Djebbar, T. Sehili, Etude cinétique de l'adsorption d'un colorant cationique (vert de méthyle) sur du charbon actif en milieu aqueux (Kinetic study of the adsorption of a cationic dye (methyl green) on activated carbon in an aqueous medium), *Sci. Technol. A* 27 (2008) 57–62.

- [38] E. Demirbas, M. Kobay, M.T. Sulak, Adsorption kinetics of a basic dye (Astrazon Yellow 7 GL) from aqueous solutions onto apricot stone activated carbon, *Biore-sour. Technol.* 99 (2008) 5368–5373.
- [39] M. Jerald Antony Joseph, N. Xavier, Equilibrium isotherm studies of MB from aqueous solution onto activated carbon prepared from *strychnos potatorium* seed, *Int. J. Appl. Biol. Pharm. Technol.* V3(3) (2012) 27–31.
- [40] G.T. Faust, J.C. Hathaway, G.A. Millot, Restudy of stevensite and allied minerals, *Am. Mineral.* 44 (1959) 342–370.
- [41] E. Voudrias, K. Fytianos, E. Bozani, Sorption–desorption isotherms of dyes from aqueous solutions and wastewaters with different sorbent materials, *Global Nest Int. J.* 4 (2002) 75–83.
- [42] T.W. Weber, R.K. Chackravorti, Pore and solid diffusion models for fixed bed adsorbers, *AIChE J.* 20 (1974) 228–238.
- [43] D. Suteu, D. Bilba, Equilibrium and kinetic study of reactive dye Brilliant Red HE-3B adsorption by activated charcoal, *Acta Chim. Slov.* 52 (2005) 73–79.
- [44] R.J. Stephenson, J.B. Sheldon, Coagulation and precipitation of a mechanical pulping effluent: 1. Removal of carbon and turbidity, *Water Res.* 30 (1996) 781–792.
- [45] F. Mogaddasi, M. Momen Heravi, M.R. Bozorgmehr, P. Ardalant, T. Ardalant, Kinetic and thermodynamic study on the removal of methyl orange from aqueous solution by adsorption onto camel thorn plant, *Asian J. Chem.* 22(7) (2010) 5093–5100.
- [46] N. Bouchamel, Z. Merzougui, F. Addoun, Adsorption en milieu aqueux de deux colorants sur charbons actifs a base de noyaux de date (Adsorption in aqueous medium of two dyes on activated carbon derived from date stones), *J. Soc. Alger. Chim.* 21(1) (2011) 1–14.
- [47] L.M. Cotoruelo, M.D. Marqués, F.J. Díaz, J. Rodríguez-Mirasol, J.J. Rodríguez, T. Cordero, Equilibrium and kinetic study of Congo Red adsorption onto lignin-based activated carbons, *Transp. Porous Med.* 83 (2010) 573–590.